Published in final edited form as:
J Comp Neurol. 2012 November 1; 520(16): 3786–3802. doi:10.1002/cne.23168.

Bipolar Cell-Photoreceptor Connectivity in the Zebrafish (*Danio rerio*) Retina

Yong N. Li[1,*], **Taro Tsujimura**[2], **Shoji Kawamura**[2], and **John E. Dowling**[1]

[1]Department of Molecular and Cellular Biology, Harvard University, Cambridge, MA 02138

[2]Department of Integrated Biosciences, Graduate School of Frontier Sciences, the University of Tokyo, Kashiwa 277-8562, Japan

Abstract

Bipolar cells convey luminance, spatial and color information from photoreceptors to amacrine and ganglion cells. We studied the photoreceptor connectivity of 321 bipolar cells in the adult zebrafish retina. 1,1'-Dioctadecyl-3,3,3',3'-tetramethylindocarbocyanine perchlorate (DiI) was inserted into whole-mounted transgenic zebrafish retinas to label bipolar cells. The photoreceptors that connect to these DiI-labeled cells were identified by transgenic fluorescence or their positions relative to the fluorescent cones, as cones are arranged in a highly-ordered mosaic: rows of alternating blue- (B) and ultraviolet-sensitive (UV) single cones alternate with rows of red- (R) and green-sensitive (G) double cones. Rod terminals intersperse among cone terminals. As many as 18 connectivity subtypes were observed, 9 of which – G, GBUV, RG, RGB, RGBUV, RGRod, RGBRod, RGBUVRod and RRod bipolar cells – accounted for 96% of the population. Based on their axon terminal stratification, these bipolar cells could be further sub-divided into ON, OFF, and ON-OFF cells. The dendritic spread size, soma depth and size, and photoreceptor connections of the 308 bipolar cells within the 9 common connectivity subtypes were determined, and their dendritic tree morphologies and axonal stratification patterns compared. We found that bipolar cells with the same axonal stratification patterns could have heterogeneous photoreceptor connectivity whereas bipolar cells with the same dendritic tree morphology usually had the same photoreceptor connectivity, although their axons might stratify on different levels.

Keywords

DiI; photoreceptors; bipolar cells; retina; connectivity; zebrafish

Introduction

Bipolar cells receive input from photoreceptors (rods and cones) in the outer retina and transmit signals to amacrine and ganglion cells in the inner retina. In the outer plexiform layer (OPL) of the retina, bipolar cells connect to photoreceptors with two types of synapses – ribbon synapses and flat (or basal) contacts, mediating sign-reversing and sign-preserving

*Correspondence to Yong N. Li, Department of Molecular and Cellular Biology, 16 Divinity Avenue, BL2081, Cambridge, MA 02138, Phone: (617) 495-2599, Fax: (617) 496-3321, yongli@mcb.harvard.edu.

Conflict of interest statement

The authors have no conflict of interest.

Role of authors

Study concept and design: Y.N.L. and J.E.D. Acquisition, analysis and interpretation of data: Y.N.L. Providing the SWS1-GFP, SWS2-GFP, and LWS-GFP fish via the National Bioresource Project of Japan: T.T. and S.K. Drafting and revision of the manuscript: Y.N.L. and J.E.D. All authors read and approved the final manuscript.

responses to light, respectively (Dowling, 2012). In the inner plexiform layer (IPL), bipolar cell axon terminals/varicosities are either mono- or multi-stratified. Nine to seventeen morphological types of bipolar cells have been described in vertebrates including cat (Kolb et al., 1981), rabbit (MacNeil et al., 2004), mouse (Ghosh et al., 2004; Wässle et al., 2009), monkey (*Macaca Mulatta*) (Boycott and Wässle, 1991; Joo et al., 2011), human (Kolb et al., 1992), pigeon (Mariani, 1987), turtle (*Pseudemys scripta elegans*) (Kolb, 1982; Ammermüller and Kolb, 1995), salamander (*Ambystoma tigrinum*) (Wu et al., 2000), rudd fish (*Scardinius erythrophthalmus*) (Scholes, 1975), goldfish (*Carassius auratus*) (Ishida et al., 1980; Sherry and Yazulla, 1993), and zebrafish (*Danio rerio*) (Connaughton et al., 2004).

Based on their responses to white light spots presented to the centers of their receptive fields, bipolar cells are classified as ON or OFF cells: OFF cells hyperpolarize whereas ON cells depolarize to the light spots (Werblin and Dowling, 1969; Kaneko, 1970). There are also some bipolar cells that response to a white light stimulus with both ON and OFF components (Wu et al., 2000; Wong and Dowling, 2005). A bipolar cell's ON or OFF center respond to white light stimulus has been found to correlate with its axonal stratification in the IPL: OFF cells' axonal varicosities are located in the outer part of the IPL (OFF sublamina) and ON cells' axonal varicosities in the proximal part of the IPL (ON sublamina) (Famiglietti et al., 1977; Nelson and Kolb, 1983; Saito et al., 1985; Euler et al., 1996; Wu et al., 2000). For those bipolar cells that have axonal varicosities in both the outer and the inner parts of the IPL, they often appear to be either ON- or OFF-cells physiologically with white light stimuli (Ammermüller and Kolb, 1995; Connaughton and Nelson, 2000; Wu et al., 2000); although some of them show both ON and OFF components in their responses to white light (Wu et al., 2000; Wong and Dowling, 2005).

When the receptive field center is stimulated with light spots of different colors, some bipolar cells respond with different polarities, i.e., they are color opponent (Kaneko, 1973; Mitarai et al., 1978; Hashimoto and Inokuchi, 1981; Kaneko and Tachibana, 1983; Ammermüller et al., 1995; Shimbo et al., 2000; Wong and Dowling, 2005). In terms of mechanisms that form center color opponency in bipolar cells, the results of two studies are informative. Haverkamp et al. (1999) examined the photoreceptor synapses of a color-opponent red-ON, blue/green OFF bipolar cell in the turtle retina by electron microscopy. They found that this bipolar cell type made ribbon synapses with red cones and basal contact synapses with green cones. The cell had no input from blue cones. The other study by Wong et al (2005) examined the glutamate receptors and light-evoked responses of multi-stratified cone-connecting bipolar cells in the giant danio (*Devario aequipinnatus*) retina. They found that a number of these multi-stratified bipolar cells responded to short and long (i.e., 430 nm and 550 nm, or 460 nm and 640 nm) wavelengths of lights with sustained potentials of opposite polarity. The depolarizing potentials could be blocked by antagonists inhibiting postsynaptic receptors at ribbon synapses, whereas the hyperpolarizing potentials were blocked by antagonists to postsynaptic receptors at basal contacts.

However, as there are many bipolar cell types, how are the various bipolar cells connected to specific photoreceptors? To answer this question, positive identification of the photoreceptor types to which each bipolar cell connects is required. The zebrafish (*Danio rerio*) retina provides an advantageous system for photoreceptor identification. It has five types of photoreceptors: double cones, consisting of a red-sensitive (R) principal member (long-double cone) and a green-sensitive (G) accessory member (short-double cone); blue-sensitive (B) long single cones; ultraviolet-sensitive (UV) short single cones; and rods. The position of each cone subtype is precisely arranged relative to the others, forming a highly ordered mosaic in which rows of alternating B and UV cones alternate with rows of R and G cones (Robinson et al., 1993). Therefore, if the location of one or two of the four types of cones in the double/single cone rows is known, the location of the other types of cones can be determined (Li et al., 2009). Transgenic zebrafish lines are now available to identify UV, B and R cones (Takechi et al., 2003; Takechi et al., 2008; Tsujimura et al., 2010) as well as rods (Fadool, 2003).

In this study, we inserted 1,1'-Dioctadecyl-3,3,3',3'-tetramethylindocarbocyanine perchlorate (DiI) into whole-mounted transgenic zebrafish retinas and observed DiI-labeled bipolar cells distal from the insertion site. We examined 321 DiI-labeled bipolar cells for their photoreceptor connectivity by confocal microscopy. By referring to the cone terminal mosaic and using transgenic fish, we could identify the photoreceptor type(s) to which each DiI-labeled bipolar cell connected.

Materials and Methods

SWS1-GFP transgenic [Tg(zfSWS1–5.5A:EGFP)] (Takechi et al., 2003), LWS-GFP transgenic [Tg(LAR:LWS2up1.8kb:GFP)#1499] (Tsujimura et al., 2010), SWS2-GFP transgenic [Tg(zfSWS2–3.5A:EGFP)] (Takechi et al., 2008), and XOPS-EGFP transgenic (Fadool, 2003) zebrafish were intercrossed to create double transgenic lines: SWS1-GFP:LWS-GFP, SWS1-GFP:XOPS-EGFP, SWS2-GFP:XOPS-EGFP. All zebrafish lines were maintained in the Harvard University Zebrafish Facility. All protocols were approved by the Harvard University Institutional Animal Care and Use Committee and conform to National Institute of Health animal care guidelines.

Adult fish (3–14 months) were euthanized using 0.02% tricaine (Sigma Chemical Company, St. Louis, MO) in Tris buffer (pH 7.4) for 10 minutes and their spinal cord transected behind the head with a razor blade. Eyes were enucleated, and the anterior segment cut off and discarded. The eyecups were fixed in fresh 4% paraformaldehyde (Fisher Scientific, Fair Lawn, NJ) at room temperature for 1 hour or at 4°C overnight. After a 3 × 10 minute wash in phosphate-buffered saline (PBS, pH 7.4, Sigma), the sclera was peeled away and the pigment epithelium sometimes removed. The residual vitreous was carefully removed under the dissecting microscope to help flatten the retina. Four radial cuts were made to allow for further flattening. The retinas were mounted onto glass slides with the ganglion cell side facing up. For DiI staining, a 1% CellTracker™ CM-DiI (Invitrogen, Carlsbad, CA) ethanol solution was spread over a glass slide and air-dried. By scratching over the DiI layer on the slide, dry DiI powder was loaded onto the outer surface of pulled tips (2–6 μm) from 1.5 mm diameter borosilicate glass pipettes (World Precision Instruments, Inc., Sarasota, FL). One or two tips were inserted perpendicularly into the middle one-third of each quadrant of the retina through the vitreous side and broken off. Retinas were kept in PBS at 4°C for ten to fourteen days. In some cases, the retinas were also counterstained with the nuclear dye 4',6-diamidino-2-phenylindole (DAPI) 90 μM. The retinas were whole-mounted with the ganglion cell layer side up on glass slides and cover-slipped using No. 0 cover glass (VWR Scientific, Media Park, PA) in VECTASHIELD® mounting medium (Vector Labs, Burlingame, CA). Pieces of No. 1 cover glass were placed around the retinas to prevent them from being crushed during imaging.

Bipolar cells were optically sectioned at optimal thickness (0.37 μm for a 40× lens) using an upright LSM 510 Meta Axioplan 2 or an inverted LSM 700 Imaging confocal microscope (Carl Zeiss MicroImaging Inc., Thornwood, NY). FluoArc argon laser light (405 nm) and a band-pass filter (420–480 nm) were used to visualize DAPI, 488 nm laser light and a band-pass filter (505–530 nm) for GFP and 543 nm laser light and a long-pass filter (560 nm) for DiI. Three objectives were used to collect images including: a 10× Plan-NEOFLUAR objective (0.30); a 25× Plan-NEOFLUAR oil-immersion corrected objective (0.80); and a 40× Plan-NEOFLUAR Oil DIC objective (1.30).

The optical serial images of bipolar cells or their maximum pixel value projections along a single axis were analyzed using the Zeiss LSM Image Browser program (Carl Zeiss MicroImaging Inc.) (Song et al., 2008; Li et al., 2009). The depth of the soma was measured from most of the distal tips of the bipolar cell dendrites where they contact the rod and cone terminals to the center of the soma. The dendritic and soma areas were calculated from measurements of the major and minor axes, assuming they were oval in shape. Student's *t*-Test was used to calculate the statistical significances, assuming the two data sets had two-tailed distribution and unequal variance.

The optical images of bipolar cells and photoreceptors were exported by the Zeiss LSM Image Browser program into Adobe Photoshop Documents. Their contrast and brightness were adjusted in Adobe Photoshop CS5.1 (Adobe Systems Inc., San Jose, CA) and their sizes in Adobe Illustrator CS5.1 (Adobe Systems Inc., San Jose, CA). The diagrams were drawn in Adobe Photoshop CS5.1 and then adjusted in size in Adobe Illustrator CS5.1. Figures were created in Adobe Illustrator CS5.1.

Results

Photoreceptor Terminal Mosaic

The mosaic arrangements of the cone inner segments (A) along with cone and rod terminals (B–D) are shown in Figure 1. At the inner segment level, UV cones (labeled with bright fluorescence) and B cones (the "void" spaces between two vertically-aligned UV cones) form vertical single cone rows; R cones (labeled with dim fluorescence) and G cones (the "void" spaces paired with R cones) form double cone rows flanking the B and UV cones, respectively (Fig. 1A). In most sections at the photoreceptor terminal level, we observed that: 1) there was some shift between the single cone rows and the double cone rows compared to the inner segment mosaic so that R cone terminals were adjacent to the UV cone terminals (Fig. 1B–D); 2) B cones (the "void" spaces below each UV cone – dim fluorescence in Figure 1C) were not at the midpoint between two neighboring UV cones, but closer to one of the UV cones (Fig. 1C,D); 3) neighboring double cones (the "void" doublet spaces between two single cone rows in Fig. 1C) were not parallel to each other but formed a zigzag pattern (Fig. 1C, black lines in 1D); and 4) the numerous rod terminals (labeled with bright fluorescence in Figure 1C) filled in between the cone terminal mosaic (Fig. 1C,D).

At the terminal level fine processes (telodendria) are seen extending out from the UV cone terminals to contact each other (Fig. 1B) and to the locations of B cones (arrowhead in Fig. 1B). In other sections, the telodendria appear to contact other cone terminals as well. Central dark areas can be seen in the R cone terminals which likely correspond to the large central invagination typical of fish cones (Allwardt et al., 2001). They are also seen in rod terminals (Fig. 1C, arrow), B cone terminals (Fig. 4B, Fig. 5B,D) and UV cone terminals (Figs. 4D,E,H, 5F–H).

A Type Specimen Bipolar Cell and Its Photoreceptor Connectivity

In a previous study, pipette tips loaded with dry DiI powder were inserted and broken off inside the retina to stain horizontal cells (Li et al., 2009). This resulted in blooms of horizontal cells around the inserted dye (Li et al., 2009). We noted that bipolar cells were occasionally observed between the horizontal cells, and here we used the same technique to visualize bipolar cells. The dendritic tree and photoreceptor connectivity of a type specimen bipolar cell are shown in Figure 2. Bipolar cell dendrites usually end as single, double or triple terminals, or sometimes in small clusters (arrows, Fig. 2B), rather than in a rosette-like arrangement typical of horizontal cell dendritic terminals. A connection between a particular

NIH-PA Author Manuscript

NIH-PA Author Manuscript

receptor terminal and a bipolar cell was judged to exist when a DiI-labeled bipolar cell dendritic terminal ended in the same position as a photoreceptor terminal. Usually, these dendrites terminated in the central region of a cone terminal, which could be determined because the large central invagination is typically darker than the peripheral regions of the terminal (Fig. 2B). The cell in Figure 2, for example, had dendritic terminals that contacted all of the cone types. Two dendritic terminals clearly fell outside of the locations of cone terminals (Fig. 2B, arrowheads) and presumably contacted rod terminals interspersed among the cone terminals (Fig. 1C,D). We designated each bipolar cell by its photoreceptor connections, i.e., this cell was, therefore, a RGBUVRod bipolar cell.

Photoreceptor Connectivity Subtypes

Of the DiI-labeled bipolar cells imaged (~ 430 cells), 321 bipolar cells had identifiable dendritic and axon terminals, and their photoreceptor connectivity and axonal stratification could be determined. Of these, 129 cells (40%) connected only with cones (cone bipolar cells) whereas 192 cells (60%) connected with both cones and rods (mixed bipolar cells). No bipolar cell was observed to have only rod connections. In total, 18 connectivity subtypes were found among these 321 bipolar cells – RGBUV (34 cells), RG (29 cells), GBUV (27 cells), RGB (20 cells), G (15 cells), RGRod (73 cells), RGBUVRod (47 cells), RGBRod (45 cells), RRod (18 cells), GRod (3 cells), RGUVRod and GBUVRod (2 cells each), R, B, GB, GUV, GBRod and GUVRod (1 cell each). As the total number of the last nine connectivity subtypes (13 cells) accounts for only 4% of the observed bipolar cells, this report focuses on the nine common subtypes (308 cells in total). The five common cone bipolar cell subtypes (RGBUV, RG, GBUV, RGB and G) make up 97% of the cone bipolar cells and the four common mixed bipolar cell connection subtypes (RGRod, RGBUVRod, RGBRod and RRod) make up 95% of the mixed bipolar cells. If we arrange these 9 common subtypes by their absolute numbers, RGRod > RGBUVRod > RGBRod > RGBUV > RG > GBUV > RGB > RRod > G. It is important to note that the connectivity categorization in this analysis was strict; one rod or cone connection would categorize a bipolar cell as connecting to that photoreceptor.

Bipolar Cell Axonal Stratification Analysis

Among the 308 bipolar cells, 184 cells (60%) were mono-stratified, 99 cells (32%) bi-stratified and 25 cells (8%) tri-stratified (Table 1). The IPL in the retina is often divided into 6 equal strata, s1-s6, although this is arbitrary and in some species as many as 10–12 strata are thought to exist (Scholes, 1975; Wu et al., 2000; Roska and Werblin, 2001; Connaughton et al., 2004; Pang et al., 2004). It is generally agreed that s1-s3 in the fish IPL represent the OFF sublamina, whereas s4-s6 encompass the ON sublamina. Out of the 184 mono-stratified bipolar cells, 118 cells (64%) terminated in s1-s3 and 66 cells (36%) in s4-s6 (Table 1). Therefore, of the 184 mono-stratified bipolar cells 118 cells were likely OFF cells and 66 ON cells. Among the 99 bi-stratified bipolar cells, 47% (47 cells) had both of their axonal varicosities located in the OFF sublamina; 8% (8 cells) had both varicosities in the ON sublamina; and 44% (44 cells) had one varicosity in the OFF sublamina and the other in the ON sublamina. Of the 25 tri-stratified bipolar cells, 17 cells (68%) had their axonal varicosities in both OFF and ON sublaminae; 8 cells (32%) had all their three varicosities located in the OFF sublamina.

Of the 57 mono-stratified cone bipolar cells, 30 cells (53%) terminated in s3 or s4. In contrast, only 26 out of the 144 mono-stratified mixed bipolar cells (18%) terminated in s3 or s4. Out of 12 axonal stratification patterns for the bi-stratified bipolar cells, the most common combination for the cone bi-stratified bipolar cells was s3s5 (38%), whereas the most common combination for the mixed bi-stratified bipolar cells was s1s3 (44%). Out of 9 axonal stratification patterns for the tri-stratified bipolar cells, the most common pattern for the cone cells was s1s3s5 (58%) and for the mixed cells, s1s2s3 (54%).

Distribution of the 9 common connectivity subtypes in the 11 major stratification patterns ($n \geq 7$) is shown in Table 2. Except for RRod bipolar cells, all the other 8 common connectivity subtypes had multiple stratification patterns, with great variation however. For example, of 71 RGRod bipolar cells, 23 cells (32%) stratified in s1 only, 16 cells (23%) in s2 only, 12 cells (17%) in s5 only, and no cell had the s1s3 pattern which was the most common stratification pattern for the RGBUV and RGBUVRod cells (Table 2). RRod cells had only one stratification pattern, s6 (18 cells, 100%).

OFF, ON and ON-OFF Distribution within Each Common Connectivity Subtype

Of the 308 cells of the 9 common connectivity subtypes there were 173 OFF, 74 ON, and 61 ON-OFF bipolar cells, an approximate ratio of 12:5:4. However, the OFF:ON:ON-OFF ratio for different connection subtypes varied (Fig. 3). For example, for GBUV bipolar cells, the ratio was 2:1:6 ($n = 27$) and for RGBUVRod bipolar cells, it was 6:1:1 ($n = 47$). Two exceptional cases were the G and RRod bipolar cells which were all OFF or ON cells, respectively. ON-OFF cells, many of which may be involved in color processing (Wong and Dowling, 2005), consisted of 67% GBUV, 28% RG, 35% RGB and 29% RGBUV bipolar cells.

Morphometry of the 308 Bipolar Cells

The bipolar cells of the 9 common connectivity subtypes had various sized dendritic spreads with an average of 657 μm^2 (Table 3). When connectivity subtypes were compared in terms of dendritic spread size, G, RGBRod and RGRod subtypes had different average spread sizes ($p < 0.05$). On average, G bipolar cells had the largest average dendritic spread size (2610 μm^2) while RGRod bipolar cells the smallest (431 μm^2). The 74 ON bipolar cells had smaller dendritic spread sizes than the 61 ON-OFF bipolar cells (548 μm^2 vs. 688 μm^2 on average, $p < 0.05$). Within each common subtype other than the G and RRod subtypes, the OFF, ON and ON-OFF cells could have quite different average dendritic spread sizes. For example, the average dendritic spread size of the ON-OFF RGBUVRod bipolar cells was 1196 μm^2, twice as big as those of the OFF and ON RGBUVRod bipolar cells ($p < 0.05$).

The average soma size for the 308 bipolar cells was 39 μm^2 with a range of 21–80 μm^2 (Table 3). The 125 cone bipolar cells had significant different soma sizes from the 183 mixed bipolar cells (37 μm^2 vs. 41 μm^2 on average, $p < 0.05$). However, there was no significant difference between the cone bipolar cells and the mixed bipolar cells when RRod bipolar cells were excluded ($p > 0.05$). Among the 9 common connectivity subtypes, RRod bipolar cells had the largest soma sizes (36–80 μm^2, or 53 μm^2 in average) and RGB bipolar cells the smallest (25–49 μm^2, or 35 μm^2 on average, $p < 0.05$). Although G bipolar cells had a larger average soma size than the other cone bipolar cells, the difference was not statistically significant ($p > 0.05$). In general, the ON bipolar cells ($n = 74$) had larger soma sizes than the OFF cells ($n = 173$) and the ON-OFF cells ($n = 61$) (43 μm^2 vs. 39 μm^2 and 37 μm^2 on average, $p < 0.05$). Within the RGBRod subtype, the ON-OFF cells had significant smaller soma sizes than the OFF cells (32 μm^2 vs. 40 μm^2 on average, $p < 0.05$). Correlating with their large soma sizes, RRod bipolar cells also had thicker axons than the bipolar cells of other connectivity subtypes, probably reflective of their large soma sizes.

Soma depth varied from 5 to 28 μm with an average of 12 μm for the 308 bipolar cells (Table 3). OFF cells were most proximal (5–23 μm, or 11 μm on average), ON cells deepest (7–28 μm, or 14 μm on average) and ON-OFF cells in between (7–26 μm, or 13 μm on average). The differences in soma depth between the OFF cells and ON or ON-OFF cells were significant ($p < 0.05$). However, within each common subtype other than the G and RRod subtypes, the OFF, ON and ON-OFF cells had no significant difference in soma depth ($p > 0.05$). When each connectivity subtype was compared with the rest of the 308 bipolar cells in soma depth, GBUV, RGRod and RRod subtypes showed significant differences. GBUV bipolar cells had the deepest soma locations that ranged from 9 to 24 µm (16 µm on average), and RGRod bipolar cells were most proximal (5–22 µm, or 12 µm on average).

Quantification of the Bipolar Cells' Photoreceptor Connections

The average number of different photoreceptor connections for the 308 bipolar cells was 6 R, 8 G, 2 B, and 1 UV cones and 8 rods (Table 4). For the various connectivity subtypes, the average photoreceptor connections varied. For example, GBUV cells connected on average to 8 G, 4 B and 5 UV cones, and RGB cells to 7 R, 11 G and 3 B cones. From the cone connection counts, we could calculate the ratios among the bipolar cell subtypes. In the cone mosaic of the zebrafish retina, the R:G:B:UV ratio is 2:2:1:1 (Robinson et al., 1993; Allison et al., 2010). If a bipolar cell or a group of bipolar cells connects to certain cone types selectively, then the ratio between connections for each cone type will deviate from the "default" R:G:B:UV ratio of 2:2:1:1. For example, the RGBUVRod bipolar cell in Figure 2 connected to 7 R, 14 G, 7 B and 4 UV cones and so they were in an approximate 2:4:2:1 ratio, which suggested that this bipolar cell connected less often with R and UV cones than the default ratio. For the 9 common bipolar cell connectivity subtypes, an average RGBUVRod (7:9:4:4), GBUV (8:4:5), RG (7:9), and RGRod (8:7) cell had approximately the default ratios. On the other hand, an average RGB cell (7:11:3) had a higher G cone ratio than the default ($p < 0.05$); and an average RGBUV cell (5:7:4:4) had a lower R cone ratio than the default ($p < 0.05$). These data clearly indicate that bipolar cells are selective in terms of the cone types they connect to.

The total number of cones to which a bipolar cell connected was counted (Table 4). On average, a bipolar cell connected to 18 cones. When bipolar cells of each connectivity subtype were compared to the rest of the 308 bipolar cells, RGB (21 cones), RGBUV (21 cones), RGBUVRod (24 cones), RGRod (15 cones) and RRod (9 cones) showed significant differences ($p < 0.05$). Differences were also observed between GBUV ON and OFF cells (10 vs. 20 cones), GBUV ON and ON-OFF cells (10 vs. 17 cones), RGBRod ON and OFF cells (20 vs. 16 cones), and RGBRod ON and ON-OFF cells (20 vs. 14 cones) ($p < 0.05$ for all).

Because a larger number of cones to which a bipolar cell connected could be due simply to this bipolar cell having a larger dendritic field, the total number of cones should be normalized by the dendritic spread area. Therefore, the ratio between the total numbers of cones to which a bipolar cell connected and the cell's dendritic spread area was determined (Table 4). The average ratio for all of the 308 cells was 0.04. As expected, G and RRod bipolar cells had the smallest cone count/dendritic area ratios as they connected to only one type of cone within their dendritic field; and RGBUV and RGBUVRod bipolar cells had the largest ratios as they connected to all types of cones within their dendritic spread ($p < 0.05$). RG and RGBRod bipolar cells also showed differences in terms of this ratio ($p < 0.05$). However, among the ON, OFF and ON-OFF cells of each connectivity subtype, differences were observed only between RGB OFF and ON-OFF cells, and RGBUVRod OFF and ON-OFF cells, indicating RGB and RGBUVRod OFF and ON-OFF cells sample cones differently within their dendritic fields.

Some Typical Cone Bipolar Cell Dendritic Tree Morphologies

G bipolar cells had elongated dendritic trees and demonstrated two dendritic tree morphologies (Fig. 4A,B). Both had the largest dendritic spreads of all the bipolar cells with thin and bifurcating dendrites, and they contacted G cone terminals usually with single or double dendritic terminals. However, the G bipolar cell shown in Figure 4A had smooth dendrites (a smooth G bipolar cell), whereas the one shown in Figure 4B had varicosities along its dendrites (a rough G bipolar cell). Interestingly, the smooth G bipolar cells usually connected to the G cone terminals closer to the cell body whereas the rough G bipolar cells did the opposite – they connected to G cone terminals further from the cell body.

RGB bipolar cells usually had tapered wandering dendrites with varicosities, and they connected to both members of the double cones (R and G cones) and a few B cones with single or multiple dendritic terminals (Fig. 4C). GBUV bipolar cells had varicosities proximally in their dendritic trees and tapered dendrites. They contacted photoreceptor terminals with single/double or triple dendritic terminals (Fig. 4D).

RG bipolar cells had various dendritic tree morphologies (Fig. 4E–G). The cell in Figure 4E had thin and straight dendrites and contacted R and G cones mainly with multiple dendritic terminals, especially in the center of its dendritic tree. The cell in Figure 4F had bifurcating, thin dendrites, a large dendritic spread, and it connected to photoreceptor terminals mostly with single dendritic terminals. It was similar to the G bipolar cells except its dendritic tree was smaller and it contacted both R and G cone terminals. The bipolar cell in Figure 4G was similar to the one in Figure 4F except its dendrites were more wandering and it had a smaller dendritic spread.

The dendritic tree pattern in Figure 4H was observed in RGBUV bipolar cells. It shared similarities with the GBUV cell in Figure 4C as they both had tapered dendrites with varicosities and both connected to cone terminals with 1–3 dendritic terminals. It also shared similarities with the RGB cell in Figure 4D as they both had relatively smooth and wandering dendrites. However, the RGBUV cell usually contacted cone terminals with one, two or occasionally 3 dendritic terminals, in contrast with the RGB cell which typically connected with a cone terminal with multiple (≥ 3) dendritic terminals. The dendritic tree of the RGBUV cell in Figure 4H was also very similar to that of the RGBUVRod bipolar cell in Figure 2 except that it had no rod connections.

Some Typical Mixed Bipolar Cell Dendritic Tree Morphologies

Some common dendritic tree patterns observed in the mixed bipolar cells are shown in Figure 5. Compared to cone bipolar cells shown in Figure 4, most of these cells had more dendritic terminals, which likely reflected their connectivity with numerous rod terminals.

Figures 5A–C show three dendritic tree morphologies observed in RGBRod bipolar cells. The RGBRod bipolar cell in Figure 5A had a stout primary dendrite from which most of the secondary dendrites branched. The secondary, tertiary and quaternary dendrites were thin and even in diameter. “Spine-like” dendritic terminals branched out from tertiary and quaternary dendrites to contact with R and G cone terminals with multiple dendritic terminals and to B cone and rod terminals with a single dendritic terminal. The RGBRod bipolar cell in Figure 5B was similar to the one in Figure 5A but it had more and smoother secondary and tertiary dendrites and fewer “spine-like” dendritic terminals branching out from each dendrite to cover its dendritic field. The RGBRod cell in Figure 5C had stiff appearing, tapered dendrites with varicosities. The RGBRod bipolar cells shown in Figure 5C (n = 3) had the second largest number of rod connections (20–36), a large soma size (43–63 μm^2) and dendritic spread area (623–872 μm^2), and their axons stratified with lobular varicosities in s1 and s2 (Fig. 6G) or, in the case of one cell, in s1, s2 and s3.

For comparison, another RGBUVRod bipolar cells is shown in Figure 5D. Similar to the cell in Figure 2, it had tapered dendrites with varicosities. It connected to the cone terminals at the center of its dendritic spread with multiple dendritic terminals but to those at the periphery with single or double dendritic terminals.

The RGRod cell in Figure 5E appeared similar to the RGBRod cell in Figure 5A except that it did not have connections with the B cone terminals. In contrast, the RGRod cell in Figure 5F appeared quite different – it had a larger dendritic spread and fewer dendritic terminals localized to the R and G cone terminals.

RRod bipolar cells had the thickest dendrites and the largest number of rod connections (30–50) among the observed bipolar cells. They typically had a stout primary dendrite, thick secondary and tertiary dendrites and many "spine-like" dendritic terminals sprouting from both the thick and the thin dendrites to connect to rods or R cone terminals (Fig. 5G). An image of its rod connecting dendritic terminals is shown in Figure 5H.

Some Typical Bipolar Cell Axonal Stratification Patterns

Some typical axonal stratification patterns of the 308 bipolar cells are shown in Figure 6. These cells were imaged from different retinas; however, each panel was adjusted to be the same magnification; the IPL was determined in each case as between the borders of the inner nuclear and ganglion cell layers. The IPL varied in thickness depending on retinal area and age of the fish. In panels A and O, six equidistant strata (s1–6) are shown, and the strata in which the bipolar cell terminals were observed are indicated below each panel. Axonal varicosities were mostly nodular (Fig. 6B,C,E,F,H–O), but sometimes disk-like (Fig. 6D), in shape. Within a single stratum, a bipolar cell often had a single axonal varicosity (Fig. 6B–F,H,I,M–O), sometimes with small branches (Fig. 6J,K), or lobular varicosities (Fig. 6A,G,L).

No Consistent Correlation between Dendritic Tree Morphology and Axonal Stratification Pattern

As some of the bipolar cell subtypes such as G, RG and RGBRod bipolar cells have more than one dendritic tree morphology, is there a correlation between their dendritic tree morphology and axonal stratification pattern? For some bipolar cells this may be so. For example, all of the 18 RRod bipolar cells in this study terminated in s6 of the IPL; 5 of the 7 bi-stratified G bipolar cells had a "smooth" dendritic tree whereas 7 out of the 8 mono-stratified G bipolar cells had a "rough" dendritic tree. Out of the three RGBRod bipolar cells that had the dendritic tree morphology in Figure 5C, two cells stratified in s1 and s2 and one in s1–3. However, bipolar cells with the same dendritic tree morphology could also have different axonal stratification patterns. For example, Figures 7A,B show two RGRod cells with the same dendritic tree morphology, and they had comparable soma sizes and soma locations; however, one cell's axon terminated in s1 (Fig. 7a) whereas the other cell's axon in s4 (Fig. 7b).

Discussion

We began this study with the expectation that the connectivity patterns of bipolar cells with photoreceptors in the zebrafish retina would be such that we could correlate them with what is known about the physiology of fish bipolar cells. This was the case with our analysis of photoreceptor-horizontal cell connectivity in zebrafish which enabled us to provide a model that may explain the responses of horizontal cells to lights of different wavelengths (Li et al., 2009). However, the variety of connectivity patterns we observed, as well as the variability in other aspects of bipolar cell morphology in relation to the connectivity patterns, have left us without clear conclusions in this regard.

There are certain statements that we can make: First, the largest bipolar cells in terms of soma size are those that connect mainly to rods (55 rods on average) although these cell have some red cone input as well (9 ± 2 R cones). Further these RRod cells all terminate deep in the ON sublamina of the IPL, in s6. Second, we observed three RGBRod OFF cells that receive their input predominantly from rods (20–36 rods) while connecting on average to 11 R, 11 G and 3 B cones. They have a unique dendritic tree shown in Fig. 5C, large soma sizes and dendritic spread sizes, and terminate in the OFF sublamina in s1 and s2 (one cell in s1, s2 and s3) with lobular varicosities. Third, there appears to be a pure OFF-bipolar cell in zebrafish that, surprisingly, receives all of its input from green cones and terminates mainly in s3. Curiously this bipolar cell has by far the largest dendritic spread of all the bipolar cells in the retina.

The other bipolar cells have mixed input from various cones and in some cases rods, although the rod input in no case is as great as the cone input (6–9 rods on average). A minority of bipolar cells (3 subtypes) also receive input from UV cones, although again none of these bipolar cells receives its input predominantly from the UV cones. A recent study from our laboratory found that whereas larval zebrafish are positively phototaxic to visible light, they are negatively phototaxic to UV light, especially in the first 8 days after fertilization (Nava and Dowling, in preparation). These results might suggest there is a bipolar cell with predominantly UV input or all UV input, but this is not the case. It is possible that such bipolar cells exist in the larval retina but not in the adult.

Examination of the sublaminae in which the various connectivity types terminated showed considerable variability as well. Most showed terminals ending in both the ON and OFF sublaminae. Figure 8 summarizes the findings of this study. This summary figure, similar to the summary figure drawn by Scholes (1975) for the rudd retina, shows the photoreceptors to which the various bipolar cells connect as well as relative average dendritic spread size, soma size and soma depth and major axonal stratification patterns for each of the 9 common bipolar cell connectivity subtypes.

In the discussion that follows, we comment on our findings in relation to possible technical issues, earlier findings on bipolar cells in fish, and the relationships, or lack thereof, between axonal stratification, dendritic tree patterns and photoreceptor connectivity.

“Real” or “Error” Photoreceptor Connections

In this study, we saw bipolar cells connected to only one or two photoreceptor terminals of a specific type. Should these connections be counted as “real” connections or “errors” as was suggested by Scholes (1975) in his study on the bipolar cells in the rudd fish? For example, how many rod connections should be counted for a cone bipolar cell to be categorized as a mixed bipolar cell? In this study we used a cutoff of 1 to simplify our categorization. Would a single cone or rod input contribute to a bipolar cell’s response in zebrafish? Physiological studies on bipolar cells with only 1 or 2 connections to a certain photoreceptor type are needed to determine this.

ON, OFF and ON-OFF Bipolar Cell Distribution

Among the 308 bipolar cells we studied, OFF, ON and ON-OFF cells were 56%, 24% and 20% of the population, respectively, showing an asymmetrical distribution, especially of ON and OFF bipolar cells. Connaughton and colleagues (2004), on the other hand, observed a rather even distribution of ON and OFF bipolar cells labeled by DiI or DiO coated beads shot into zebrafish retina slices. The percentages they observed were 38%, 35% and 24% for OFF, ON and ON-OFF among 97 stained cells (Connaughton et al., 2004). Using DiI applied to the optic nerve to retro-label retinal ganglion cells in zebrafish, Mangrum et al.

(2002) reported among 85 retinal ganglions cells a ratio of OFF, ON and ON-OFF cells of 52%, 24% and 20%, respectively, a ratio similar to the present bipolar cell study. In an electrophysiological study of 156 ganglion cells in the larva zebrafish, on the other hand, percentages were reported as 11%, 29% and 56% for OFF, ON and ON-OFF ganglion cells (Emran et al., 2007), which may suggest that the distribution of these cells is different in larval fish. In a study on the bipolar cells in the rudd fish retina, Scholes (1975) found that bipolar cells that ended in the proximal strata were most frequently impregnated by the Golgi method and suggested that the Golgi impregnation might be selective for cell types within neuronal classes. The DiI method may also have selectivity.

Soma Size and Photoreceptor Connectivity

In teleost retinas, bipolar cells are usually identified as large or small cells based on their soma sizes, and it is generally believed that the large cells have both cone and rod connections and the small cells only cone connections (Stell, 1967; Parthe, 1972; Ramón y Cajal, 1972; Famiglietti et al., 1977; Sherry and Yazulla, 1993). However, Ishida and colleagues (1980) found that somata of the mixed bipolar cells in goldfish could be as small as those of the cone bipolar cells, or as much as twice the size of the small cells. Our data suggest that, even though on average the mixed bipolar cells have larger soma size than the cone bipolar cells, some of the mixed bipolar cells have somata as small as most of the cone bipolar cells, and that some of the cone bipolar cells have somata as big as most of the mixed bipolar cells. Thus, in agreement with Ishida et al.(1980), there is not an unambiguous correlation between a bipolar cell's photoreceptor connectivity and its soma size in zebrafish.

Correspondence with Bipolar Cell Subtypes in Earlier Studies

Can we correlate our bipolar cell connectivity subtypes with previously reported bipolar cell morphologies? The RRod cells have the largest soma sizes with stout primary dendrites, thick axons and the largest numbers of rod connections. They are likely to be the rod bipolar cells described by Cajal (1972) in the teleost retina, the large rod bipolar cells in the rudd fish retina (Scholes, 1975), the Mb1 cells in the goldfish retina (Sherry and Yazulla, 1993), the Mb cells in the carp retina (Famiglietti et al., 1977), the type b1 cells in the goldfish retina (Ishida et al., 1980), and the B_{on}-s6L cells in the zebrafish retina (Connaughton et al., 2004).

A group of RGRod cells such as the cell in Figure 7A have large soma sizes (43–59 μm^2) and their axons terminate in a single varicosity in s1. They are likely the Ma cells described by Sherry (1993), and the B_{off}-s1 cells described by Connaughton et al. (2004). The RGBRod cell in Figure 5C has a large dendritic spread, thick dendrites with many rod connections and a stratified axon in the outer IPL strata. It is likely the Ma-L cell described by Sherry (1993), and the B_{off}-s1/s2 cell described by Connaughton and colleagues (2004).

The RGBUVRod cell in Figure 5D has a large dendritic spread, slender and smooth dendrites and is possibly the type b3 cell described by Ishida and colleagues (1980). The RGRod cell in Figure 5F has thin dendrites, a thin axon and sparse rod connection so it is possibly the type a1 cell described by Ishida et al. (1980).

G bipolar cells are likely the accessory cone selective cells described by Scholes (1975), but they are different in their axonal stratification patterns. The G bipolar cells are also similar the C1a-W cells described by Sherry (1993) but we did not observe telodendria extending from their axon terminals as they did.

Rod and Cone Input into IPL

In the tiger salamander retina, rod-dominant axon terminals of the bipolar cells ramify along the inner and outer margins of the IPL, and the relative strength of rod input to bipolar cells decreases as the level of axon terminal ramification becomes more central in the IPL, i.e., cone signals are stronger in the middle of the IPL (Wu et al., 2000). Data in Table 1 suggests a similar arrangement in the zebrafish retina, at least for the mono-stratified bipolar cells as over half of the pure cone cells terminated in s3 and s4 in contrast to only about one fifth of the mixed cells.

The RRod bipolar cells have the largest number of rod connections compared to other mixed bipolar cells and they all terminated in s6 with large axonal varicosities, suggesting they are all ON bipolar cells. A similar stratification pattern has been described for rod bipolar cells of many other species (Kolb and Famiglietti, 1974; Sherry and Yazulla, 1993; Ammermüller and Kolb, 1995; Euler et al., 1996).

Bipolar Cell Photoreceptor Connections and Chromatic Properties

More than half of a randomly selected sample of bipolar cells in the carp retina was found to be color-coded, with either single or double opponent receptive fields (Kaneko, 1973). Shimbo and colleagues (2000) found 122 double-opponent cells out of 500 recorded bipolar cells in the carp retina, about evenly divided in terms of red light either hyperpolarizing or depolarizing the receptive field center and green-blue light eliciting the opposite polarity response in the center (Shimbo et al., 2000). What would the photoreceptor connectivity profile be for a color-opponent, chromatic bipolar cell? For example, quantification of the cone connections of the RGBUVRod bipolar cells showed an R:G:B:UV ratio of about 7:9:4:4 (Table 4) which is nearly identical to cone ratio 2:2:1:1 in the cone mosaic. This might suggest the RGBUVRod bipolar cells receive input from every cone type within their dendritic fields without selectivity. Does this mean that the RGBUVRod bipolar cells transmit luminosity rather than chromatic information from the outer retina to the inner retina? Given the existence of two types of cone-bipolar cell synapses, the answer is unclear as there may be another level of selectivity at the synaptic level, a sign-preserving flat contact or a sign-inverting ribbon synapse, between a bipolar cell and the various cone types to which it connects. So, for example, if the RGBUVRod cell connects to R and G cones with ribbon synapses and B and UV cones with flat contacts, it would be chromatic. Electron microscopy of bipolar cell photoreceptor connections is needed to suggest a bipolar cell's chromatic properties.

The existence of two types of synapses between cones and bipolar cells may be an explanation to the observation by Saito et al. (1985) in the carp retina and Sakai et al (1983) in the catfish retina that many ON bipolar cells make non-ribbon synapses with cones and many OFF bipolar cells make ribbon synapses with cones. If a bipolar cell synapses with two or more types of photoreceptors and the ON or OFF properties of the cell are assayed with white light, it is possible that a cell classified as an ON cell could make predominantly ribbon synapses with one or two cone types, but fewer non-ribbon synapses with other cone types. If a RG cell made predominately ribbon synapses with R cones and fewer non-ribbon synapses with G cones, then the cell would likely respond to white light with depolarization. Only with green light would the cell hyperpolarize. This supposition assumes that ribbon and basal junctions have approximately equal effects on postsynaptic cells which is not known. In primates, cones make twice as many basal contacts on the flat (OFF) midget bipolar cells than ribbon synapses on the invaginating (ON) midget bipolar cells, suggesting ribbon synapses have larger postsynaptic effects than do basal contacts (Kolb et al., 1969).

Axonal Stratification Pattern and Photoreceptor Connectivity

In total, 27 axonal stratification patterns were observed in this study. Nearly every combination could be found for both cone and mixed bipolar cells (Table 1). Moreover, more than one cone bipolar cell subtype could have the same axonal stratification pattern (Table 2). For example, a s1s3 axonal stratification pattern was encountered in G, GBUV, RGBUV and RGBUVRod bipolar cells. Therefore, axonal stratification is insufficient to determine a bipolar cell's photoreceptor connectivity. Indeed, present thinking suggests that in each stratum of the IPL, different combinations of bipolar, amacrine and ganglion cell subtypes interact to form the ganglion cell receptive field properties (Roska and Werblin, 2001). Thus, it is not unexpected that different bipolar cell types contribute to the same strata.

Dendritic Tree Morphology and Photoreceptor Connectivity

Compared to axonal stratification patterns and soma sizes, the dendritic tree morphologies are more informative about a bipolar cell's photoreceptor connectivity (Figs. 4 and 5). That is, most bipolar cells with different connectivity patterns have unique dendritic tree morphologies. This undoubtedly relates to the regular cone and rod terminal mosaic pattern found in the zebrafish retina. However, some bipolar cells with different photoreceptor connectivities have quite similar dendritic tree morphologies, such as the RGBRod cell in Figure 5A and the RGRod cell in Figure 5E, the RGBUV cell in Figure 4H and the RGBUVRod cell in Figure 5D. Without determining their photoreceptor connectivity, these cells might be classified as the same cell type.

Bipolar Cell Classification

This study is the first comprehensive study of bipolar cell-photoreceptor connectivity in any retina. Our data suggest neither axonal stratification nor soma size is sufficient to indicate the photoreceptor connectivity of a bipolar cell (Tables 2 and 3, Figs. 3 and 7). Further, bipolar cells with the same photoreceptor connectivity can have heterogeneous axonal stratification patterns and dendritic tree morphologies (Table 2 and Figs. 5, 6, and 7). How then, should bipolar cells be categorized? As a bipolar cell's photoreceptor connectivity indicates its input and axonal stratification its response sign (ON or OFF), a better way to define a bipolar cell may be to describe both its photoreceptor connectivity and its axonal stratification. In this case, Table 2 suggests that there are at least 33 bipolar cell subtypes in zebrafish. For example, RGB bipolar cells would be classified as RGB-s3 and RGB-s3s5 cells. The RGB-s3 cell would presumably be a pure OFF cell, whereas the RGB-s3s5 cell would likely be an ON-OFF cell and perhaps chromatic.

Summary

We have analyzed the connectivity between the bipolar cells and the five types of photoreceptors in zebrafish. Of the 321 bipolar cells studied, 96 percent could be assigned to one of the 9 subtypes. Five of these subtypes made cone connections exclusively, whereas four made both rod and cone contacts. By identifying the strata in which the terminals of the bipolar cells are found, we can suggest whether a bipolar cell type is likely to be an ON, OFF, or ON-OFF cell. Two bipolar cell types in the zebrafish retina appear to be exclusively ON or OFF cells – all of the other subtypes appear to be a mix of ON, OFF, or ON-OFF cells. In terms of the number of subtypes observed, the mixed rod-cone bipolar cells were seen more frequently than the pure cone bipolar cells (165 vs. 110 cells) in the following order: RGRod > RGBUVRod > RGBRod > RGBUV > RG > GBUV > RGB. Our observations also indicate that most bipolar cells contact selective sets of cones rather than all the cones within their dendritic fields. Except for RRod cells that only stratified in s6, each of the other common connectivity subtypes had multiple axonal stratification patterns

(Table 2). Different connectivity subtypes could have the same axonal stratification pattern, and vice versa – the same connectivity subtype could have different axonal stratification patterns.

This study represents a first step in determining the exact connectivity of the four cone types with the bipolar cells in a retina with rich color vision. Next steps will require electron microscopy to elucidate the type of synapses made – whether ribbon (sign-inverting) or basal (sign-conserving) – by a cone onto a bipolar cell subtype, and the number of synapses made by a specific cone onto the dendrites of a bipolar cell contacting that cone. Combining such exact anatomical data with physiological recordings from identified bipolar cells should tell us how the first steps of color processing occur in the retina.

Acknowledgments

The authors thank Drs. James Fadool and Pamela Raymond for providing transgenic zebrafish lines, Dr. Florian Engert for support and Dowling lab members for discussion. The authors also thank Jessica Miller, Steve Zimmerman and Karen Hurley in the Harvard Zebrafish Facility for their help in rearing and maintaining the fish, and Dave Smith and Harvard Biological Image Center for use of Harvard University confocal microscopes.

Grant support: NIH Grants EY00811, EY07145, and 1DP1OD008240.

References

Allison WT, Barthel LK, Skebo KM, Takechi M, Kawamura S, Raymond PA. Ontogeny of cone photoreceptor mosaics in zebrafish. J Comp Neurol. 2010; 518(20):4182–4195. [PubMed: 20878782]

Allwardt BA, Lall AB, Brockerhoff SE, Dowling JE. Synapse formation is arrested in retinal photoreceptors of the zebrafish nrc mutant. J Neurosci. 2001; 21(7):2330–2342. [PubMed: 11264308]

Ammermüller J, Kolb H. The organization of the turtle inner retina. I. ON- and OFF-center pathways. J Comp Neurol. 1995; 358(1):1–34. [PubMed: 7560272]

Ammermüller J, Muller JF, Kolb H. The organization of the turtle inner retina. II. Analysis of color-coded and directionally selective cells. J Comp Neurol. 1995; 358(1):35–62. [PubMed: 7560276]

Boycott BB, Wässle H. Morphological Classification of Bipolar Cells of the Primate Retina. Eur J Neurosci. 1991; 3(11):1069–1088. [PubMed: 12106238]

Connaughton VP, Graham D, Nelson R. Identification and morphological classification of horizontal, bipolar, and amacrine cells within the zebrafish retina. J Comp Neurol. 2004; 477(4):371–385. [PubMed: 15329887]

Connaughton VP, Nelson R. Axonal stratification patterns and glutamate-gated conductance mechanisms in zebrafish retinal bipolar cells. J Physiol. 2000; 524(Pt 1):135–146. [PubMed: 10747188]

Dowling, JE. The Retina: An Approachable Part of the Brain. Revised Edition. Cambridge, Mass: Belknap Press of Harvard University Press; 2012.

Emran F, Rihel J, Adolph AR, Wong KY, Kraves S, Dowling JE. OFF ganglion cells cannot drive the optokinetic reflex in zebrafish. Proc Natl Acad Sci U S A. 2007; 104(48):19126–19131. [PubMed: 18025459]

Euler T, Schneider H, Wässle H. Glutamate responses of bipolar cells in a slice preparation of the rat retina. J Neurosci. 1996; 16(9):2934–2944. [PubMed: 8622124]

Fadool JM. Development of a rod photoreceptor mosaic revealed in transgenic zebrafish. Dev Biol. 2003; 258(2):277–290. [PubMed: 12798288]

Famiglietti EV Jr. Kaneko A, Tachibana M. Neuronal architecture of on and off pathways to ganglion cells in carp retina. Science. 1977; 198(4323):1267–1269. [PubMed: 73223]

Ghosh KK, Bujan S, Haverkamp S, Feigenspan A, Wässle H. Types of bipolar cells in the mouse retina. J Comp Neurol. 2004; 469(1):70–82. [PubMed: 14689473]

Hashimoto Y, Inokuchi M. Characteristics of second order neurons in the dace retina: physiological and morphological studies. Vision Res. 1981; 21(11):1541–1550. [PubMed: 7336582]

Haverkamp S, Mockel W, Ammermüller J. Different types of synapses with different spectral types of cones underlie color opponency in a bipolar cell of the turtle retina. Vis Neurosci. 1999; 16(5): 801–809. [PubMed: 10580716]

Ishida AT, Stell WK, Lightfoot DO. Rod and cone inputs to bipolar cells in goldfish retina. J Comp Neurol. 1980; 191(3):315–335. [PubMed: 7410596]

Joo HR, Peterson BB, Haun TJ, Dacey DM. Characterization of a novel large-field cone bipolar cell type in the primate retina: evidence for selective cone connections. Vis Neurosci. 2011; 28(1):29–37. [PubMed: 21156090]

Kaneko A. Physiological and morphological identification of horizontal, bipolar and amacrine cells in goldfish retina. J Physiol. 1970; 207(3):623–633. [PubMed: 5499739]

Kaneko A. Receptive field organization of bipolar and amacrine cells in the goldfish retina. J Physiol. 1973; 235(1):133–153. [PubMed: 4778132]

Kaneko A, Tachibana M. Double color-opponent receptive fields of carp bipolar cells. Vision Res. 1983; 23(4):381–388. [PubMed: 6880036]

Kolb H. The morphology of the bipolar cells, amacrine cells and ganglion cells in the retina of the turtle Pseudemys scripta elegans. Philos Trans R Soc Lond B Biol Sci. 1982; 298(1092):355–393. [PubMed: 6127731]

Kolb H, Boycott BB, Dowling JE. A second type of midget bipolar cell in the primate retina. Philos Trans R Soc Lond B Biol Sci. 1969; 255:177–184.

Kolb H, Famiglietti EV. Rod and cone pathways in the inner plexiform layer of cat retina. Science. 1974; 186(4158):47–49. [PubMed: 4417736]

Kolb H, Linberg KA, Fisher SK. Neurons of the human retina: a Golgi study. J Comp Neurol. 1992; 318(2):147–187. [PubMed: 1374766]

Kolb H, Nelson R, Mariani A. Amacrine cells, bipolar cells and ganglion cells of the cat retina: a Golgi study. Vision Res. 1981; 21(7):1081–1114. [PubMed: 7314489]

Li YN, Matsui JI, Dowling JE. Specificity of the horizontal cell-photoreceptor connections in the zebrafish (Danio rerio) retina. J Comp Neurol. 2009; 516(5):442–453. [PubMed: 19655401]

MacNeil MA, Heussy JK, Dacheux RF, Raviola E, Masland RH. The population of bipolar cells in the rabbit retina. J Comp Neurol. 2004; 472(1):73–86. [PubMed: 15024753]

Mangrum WI, Dowling JE, Cohen ED. A morphological classification of ganglion cells in the zebrafish retina. Vis Neurosci. 2002; 19(6):767–779. [PubMed: 12688671]

Mariani AP. Neuronal and synaptic organization of the outer plexiform layer of the pigeon retina. Am J Anat. 1987; 179(1):25–39. [PubMed: 2441588]

Mitarai G, Goto T, Takagi S. Receptive field arrangement of color-opponent bipolar and amacrine cells in the carp retina. Sens Processes. 1978; 2(4):375–382. [PubMed: 755292]

Nelson R, Kolb H. Synaptic patterns and response properties of bipolar and ganglion cells in the cat retina. Vision Res. 1983; 23(10):1183–1195. [PubMed: 6649437]

Pang JJ, Gao F, Wu SM. Stratum-by-stratum projection of light response attributes by retinal bipolar cells of Ambystoma. J Physiol. 2004; 558(Pt 1):249–262. [PubMed: 15146053]

Parthe V. Horizontal, bipolar and oligopolar cells in the teleost retina. Vision Res. 1972; 12(3):395–406. [PubMed: 5021906]

Ramón, y; Cajal, S. The Structure of the Retina. Thorpe, SA.; Glickstein, M., translators. Springfield, Ill: C. C. Thomas; 1972.

Robinson J, Schmitt EA, Harosi FI, Reece RJ, Dowling JE. Zebrafish ultraviolet visual pigment: absorption spectrum, sequence, and localization. Proc Natl Acad Sci U S A. 1993; 90(13):6009–6012. [PubMed: 8327475]

Roska B, Werblin F. Vertical interactions across ten parallel, stacked representations in the mammalian retina. Nature. 2001; 410(6828):583–587. [PubMed: 11279496]

Saito T, Kujiraoka T, Yonaha T, Chino Y. Reexamination of photoreceptor-bipolar connectivity patterns in carp retina: HRP-EM and Golgi-EM studies. J Comp Neurol. 1985; 236(2):141–160. [PubMed: 4056093]

Sakai H, Naka KI. Synaptic organization involving receptor, horizontal and on- and off-center bipolar cells in the catfish retina. Vision Res. 1983; 23(4):339–351. [PubMed: 6880033]

Scholes JH. Colour receptors, and their synaptic connexions, in the retina of a cyprinid fish. Philos Trans R Soc Lond B Biol Sci. 1975; 270(902):61–118. [PubMed: 234623]

Sherry DM, Yazulla S. Goldfish bipolar cells and axon terminal patterns: a Golgi study. J Comp Neurol. 1993; 329(2):188–200. [PubMed: 8454729]

Shimbo K, Toyoda JI, Kondo H, Kujiraoka T. Color-opponent responses of small and giant bipolar cells in the carp retina. Vis Neurosci. 2000; 17(4):609–621. [PubMed: 11016579]

Song PI, Matsui JI, Dowling JE. Morphological types and connectivity of horizontal cells found in the adult zebrafish (Danio rerio) retina. J Comp Neurol. 2008; 506(2):328–338. [PubMed: 18022944]

Stell WK. The structure and relationships of horizontal cells and photoreceptor-bipolar synaptic complexes in goldfish retina. Am J Anat. 1967; 121(2):401–423. [PubMed: 4862097]

Takechi M, Hamaoka T, Kawamura S. Fluorescence visualization of ultraviolet-sensitive cone photoreceptor development in living zebrafish. FEBS Lett. 2003; 553(1–2):90–94. [PubMed: 14550552]

Takechi M, Seno S, Kawamura S. Identification of cis-acting elements repressing blue opsin expression in zebrafish UV cones and pineal cells. J Biol Chem. 2008; 283(46):31625–31632. [PubMed: 18796431]

Tsujimura T, Hosoya T, Kawamura S. A single enhancer regulating the differential expression of duplicated red-sensitive opsin genes in zebrafish. PLoS Genet. 2010; 6(12):e1001245. [PubMed: 21187910]

Wässle H, Puller C, Müller F, Haverkamp S. Cone contacts, mosaics, and territories of bipolar cells in the mouse retina. J Neurosci. 2009; 29(1):106–117. [PubMed: 19129389]

Werblin FS, Dowling JE. Organization of the retina of the mudpuppy, Necturus maculosus. II. Intracellular recording. J Neurophysiol. 1969; 32(3):339–355. [PubMed: 4306897]

Wong KY, Dowling JE. Retinal bipolar cell input mechanisms in giant danio. III. ON-OFF bipolar cells and their color-opponent mechanisms. J Neurophysiol. 2005; 94(1):265–272. [PubMed: 15758056]

Wu SM, Gao F, Maple BR. Functional architecture of synapses in the inner retina: segregation of visual signals by stratification of bipolar cell axon terminals. J Neurosci. 2000; 20(12):4462–4470. [PubMed: 10844015]

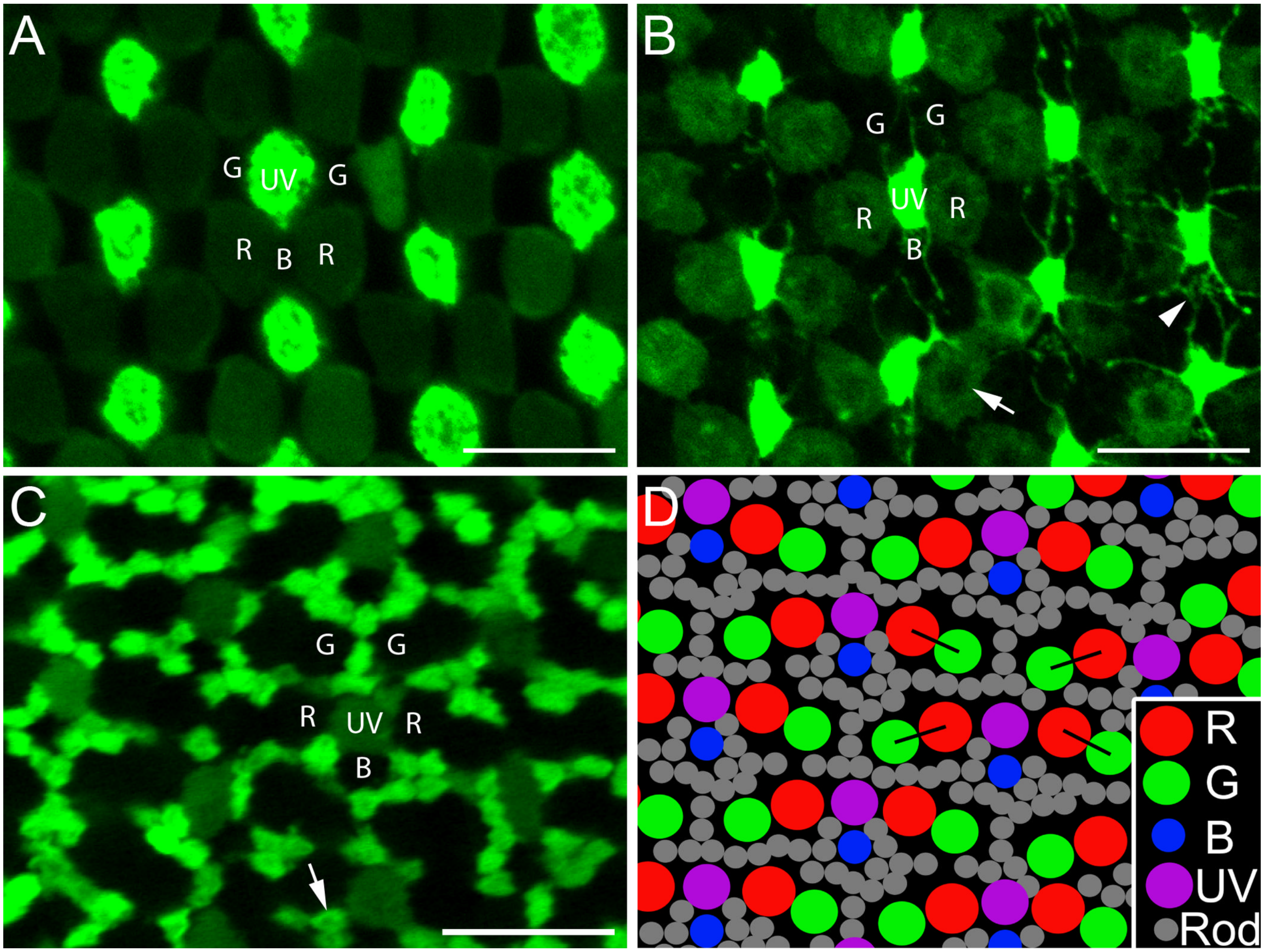

Figure 1.
The mosaic arrangements of the cone inner segments and the rod and cone terminals in the adult zebrafish retina. A,B: SWS1-GFP:LWS-GFP double transgenic retina. C: SWS1-GFP:XOPS-EGFP double transgenic retina. A: Single-plane confocal image of the cone inner segment mosaic in a SWS1-GFP:LWS-GFP retina where UV cones have bright fluorescence and R cones dim fluorescence. B: The same visual field as in A but at the level of photoreceptor terminals. Note the central dark area of the R cone terminals (arrow) which likely corresponds to the large central invagination typical of fish cones (Allwardt et al., 2001). Telodendria extend out from the UV cone terminals to contact other terminals (arrowhead). C: Single-plane confocal image of a SWS1-GFP:XOPS-EGFP retina at the photoreceptor terminals. In this micrograph UV cone terminals have dim fluorescence and rod terminals bright fluorescence, and together they delineate the locations of R, G, and B cone terminals. The rod terminal also has the central dark area (arrow). D: Diagram of the typical cone terminal mosaic along with rod terminals. The double cone (R and G) terminals form double rows and the alternating short single (UV) and long single (B) cone terminals form single vertical rows; the double rows alternate with the single rows. R cone terminals flank the UV cone terminals. Within single cone rows, the B cone terminals are not equidistant to their neighboring UV cone terminals but closer to one of them (here the upper one). Within double cone rows, the orientation of each pair of R and G cone terminals zigzags (black lines). The numerous rod terminals fill in the cone terminal mosaic. R, red-

sensitive cones; G, green-sensitive cones; B, blue-sensitive cones; UV, ultraviolet-sensitive cones; and Rod, rods. Scale bar = 10 μm.

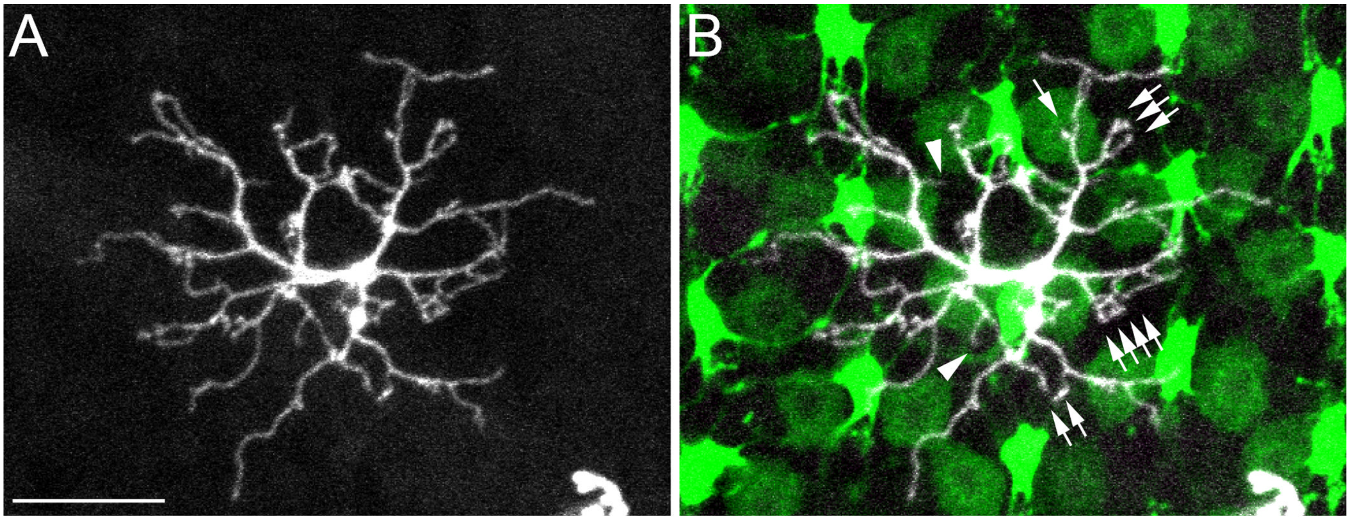

Figure 2.

A type specimen RGBUVRod bipolar cell in a SWS1-GFP:LWS-GFP double transgenic zebrafish retina. A: The z-axis projection of serial confocal images of a RGBUVRod bipolar cell showing its dendritic tree. B: Overlaying A with a single-plane confocal image of the photoreceptor terminals. UV and R cone terminals have bright and dim fluorescence, respectively. This bipolar cell connects to cone terminals with single, double, triple or more dendritic terminals (arrows). The dendritic terminals fall on R, G, B, and UV cone terminals except two that presumably connect to rod terminals (arrowheads). Scale bar = 10 µm.

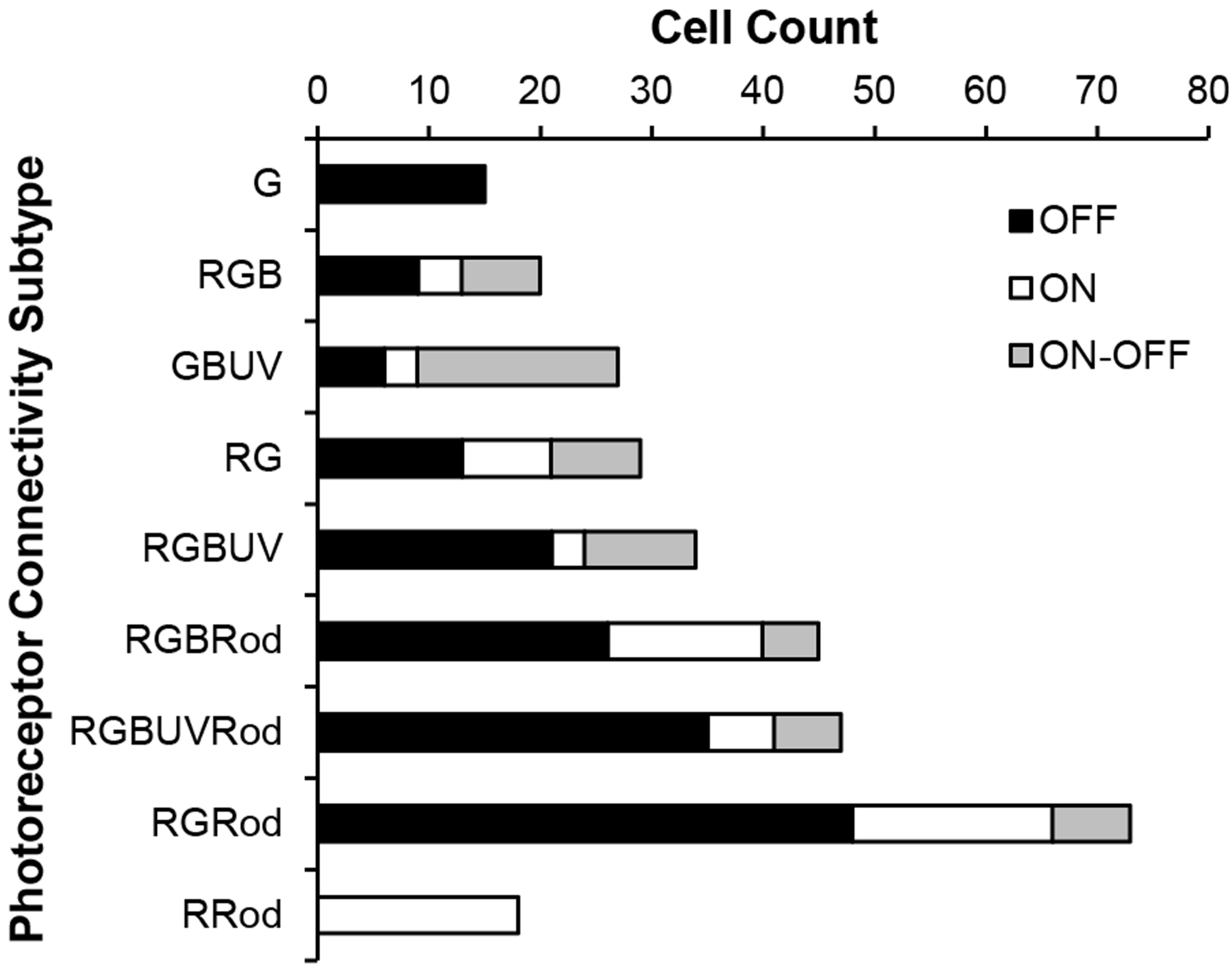

Figure 3.
The nine common connectivity subtypes and their distribution as OFF, ON and ON-OFF cells. R, red-sensitive cones; G, green-sensitive cones; B, blue-sensitive cones; UV, ultraviolet-sensitive cones; and Rod, rods. See text for details.

NIH-PA Author Manuscript

NIH-PA Author Manuscript

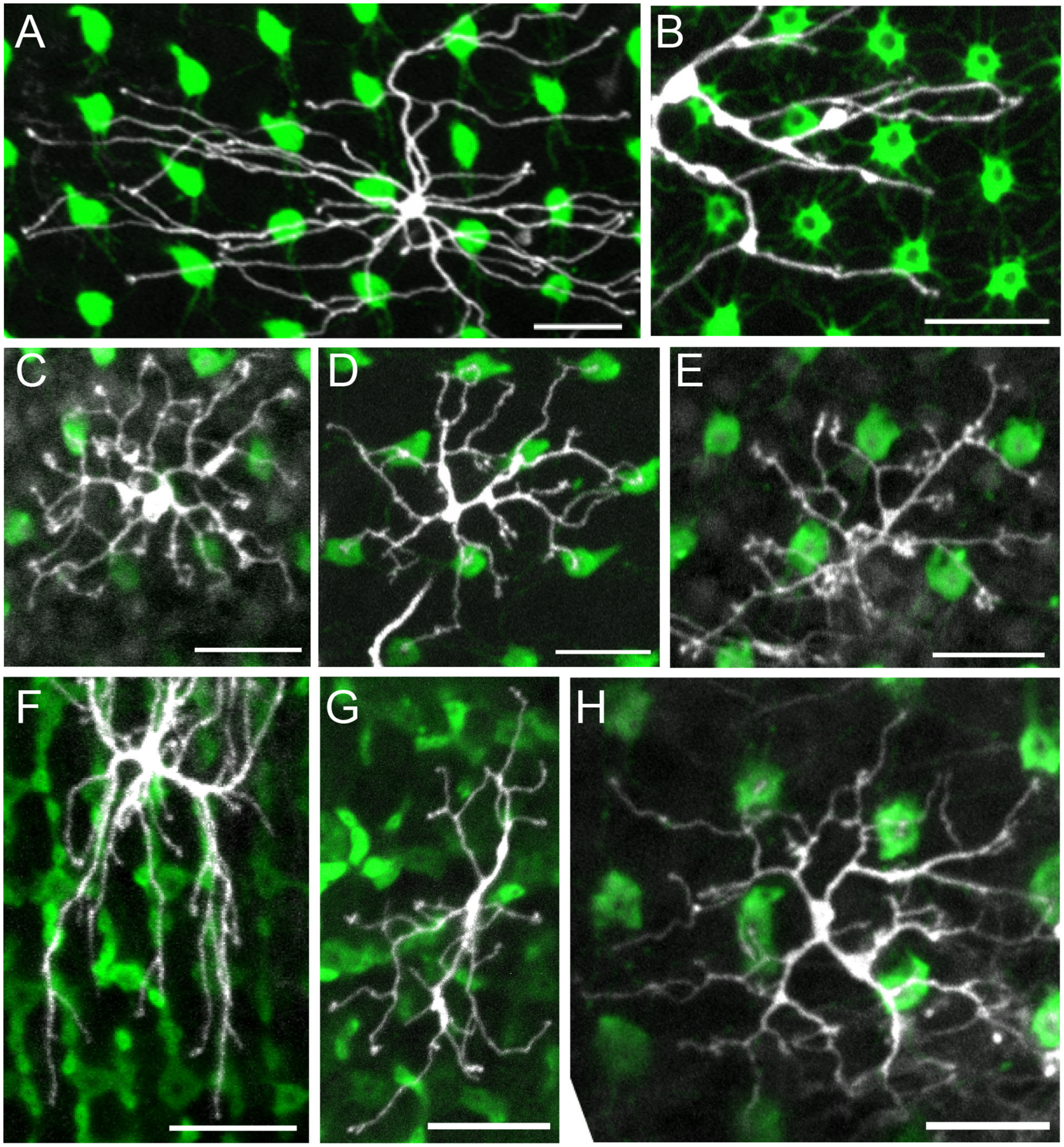

Figure 4.

Common dendritic tree morphologies of the cone bipolar cells. Each panel is the z-axis projection of serial confocal images of the dendritic tree and corresponding photoreceptor terminals. A,C–E,H: SWS1-GFP retinas, in which UV cones have bright fluorescence. B: SWS2-GFP retina, in which B cones have bright fluorescence. F: SWS2-GFP:XOPS-EGFP retina, in which both B cones and rods have bright fluorescence. G: SWS1-GFP:XOPS-EGFP retina, in which UV cones and rods have bright fluorescence. A: Partial dendritic tree of a G bipolar cell with smooth dendrites. B: Partial dendritic tree of a G bipolar cell with rough dendrites. C: Dendritic tree of a RGB bipolar cell. D: Dendritic tree of a GBUV bipolar cell. E: Dendritic tree of an RG bipolar cell with clustered dendritic terminals. F:

Partial dendritic tree of an RG bipolar cell without clustered dendritic terminals. G: Dendritic tree of an RG bipolar cell. H: Dendritic tree of an RGBUV bipolar cell. See text for details. Scale bars = 10 µm.

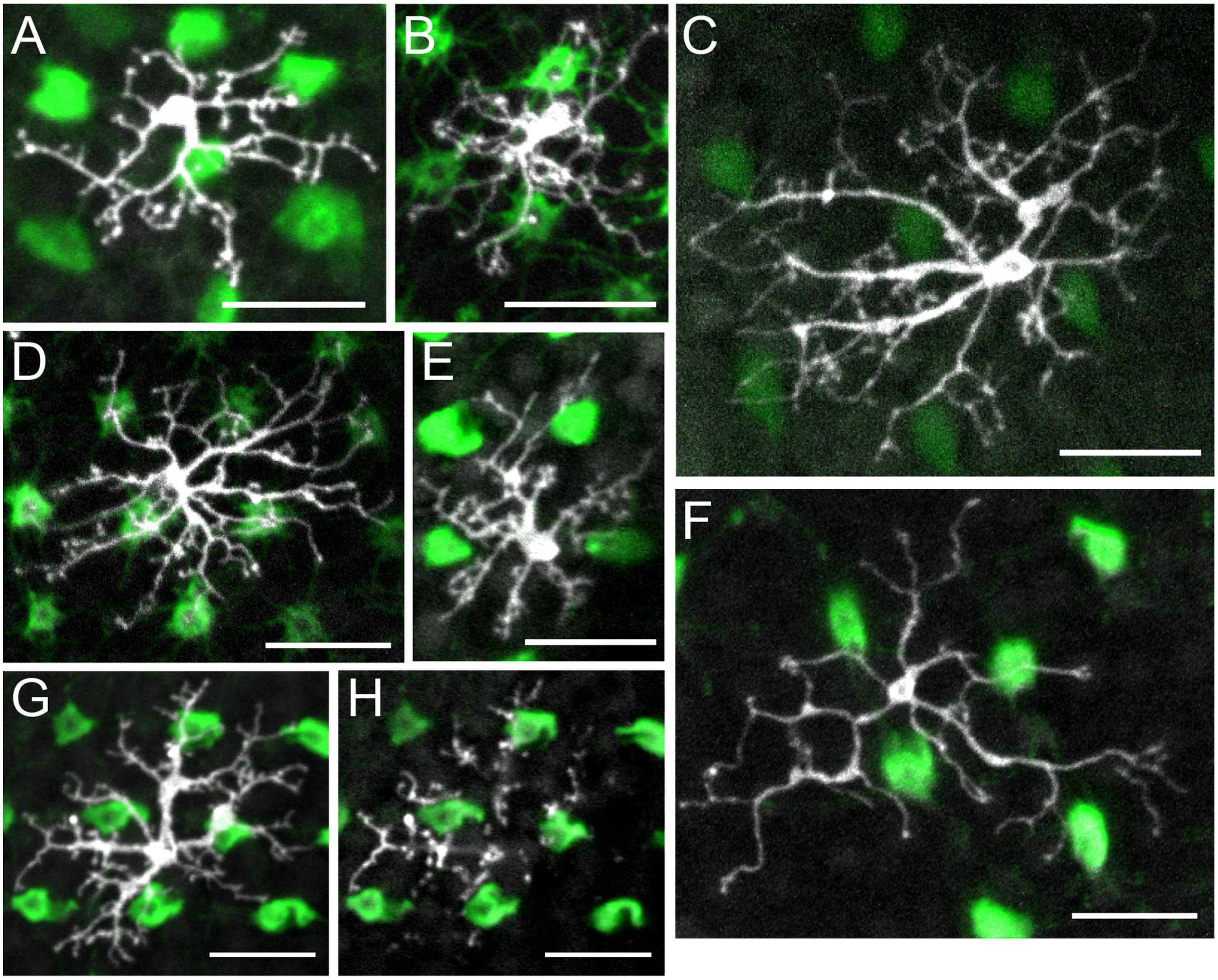

Figure 5.

Common dendritic tree morphologies of the mixed bipolar cells. A–G: The z-axis projection of serial confocal images of the dendritic tree and corresponding photoreceptor terminals. H: Single-plane image of the bipolar cell in G at its dendritic terminals and the corresponding image of the photoreceptor terminals. A,B,D: SWS2-GFP retinas, in which B cones have bright fluorescence. C,E–H: SWS1-GFP retinas, in which UV cones have bright fluorescence. A: Dendritic tree of an RGBRod bipolar cell. B: Dendritic tree of an RGBRod bipolar cell with a small dendritic spread. C: Dendritic tree of an RGBRod bipolar cell with stiff dendrites and bifurcating dendritic ends. D: Dendritic tree of an RGBUVRod bipolar cell. E: Dendritic tree of an RGRod bipolar cell with a small dendritic spread. F: Dendritic tree of an RGRod bipolar cell with smooth dendrites and only a few rod connections. G: Dendritic tree of an RRod bipolar cell. H: Dendritic terminals of the cell in G. See text for details. Scale bars = 10 μm in A–H.

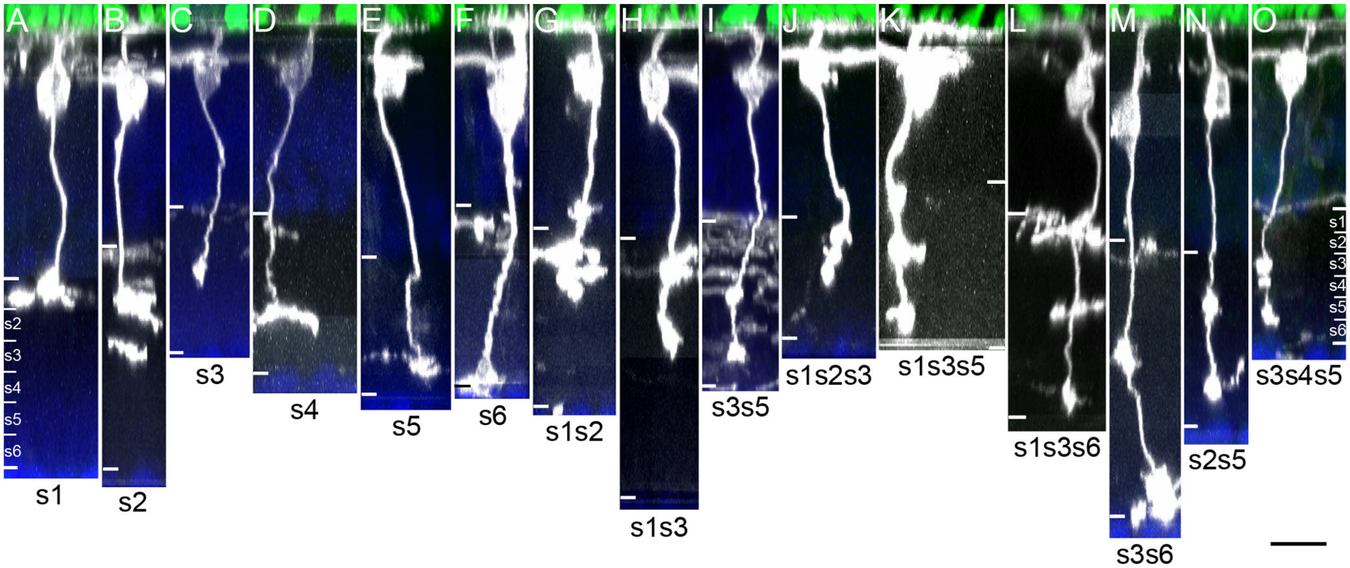

Figure 6.

Type specimens of bipolar cell axonal stratification patterns. All panels are aligned so that the transgenic cone terminals are at the same level. Borders of the IPL are marked with white lines. The IPL strata in A and O are also marked. A–J and M–O, with DAPI counter stain. A: s1. B: s2. C: s3. D: s4. E: s5. F: s6. G: s1s2. H: s1s3. I: s3s5. J: s1s2s3. K: s1s3s5. L: s1s3s6. M: s3s6. N: s2s5. O: s3s4s5. See text for details. Scale bar = 10 μm in O (applies to A–O).

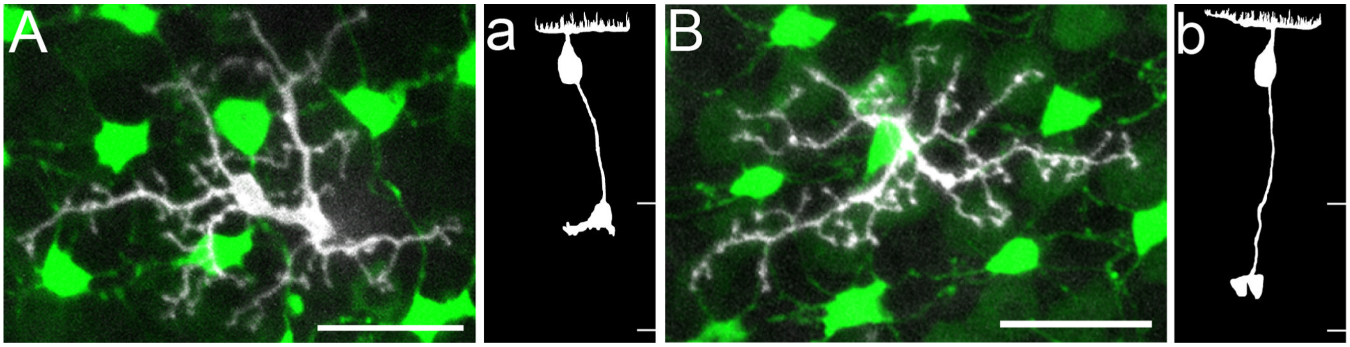

Figure 7.

Two RGRod bipolar cells with the same dendritic tree morphology and similar soma depth and size but different axonal stratification in SWS1-GFP:LWS-GFP double transgenic zebrafish retinas, in which UV and R cone terminals have bright and dim fluorescence, respectively. A,B: The z-axis projection of serial confocal images of the dendritic tree and corresponding photoreceptor terminals. a,b: Drawings in the radial plane of the bipolar cells in A and B, respectively. Borders for the IPL are marked by white lines. See text for details. Scale bars = 10 μm in A,B.

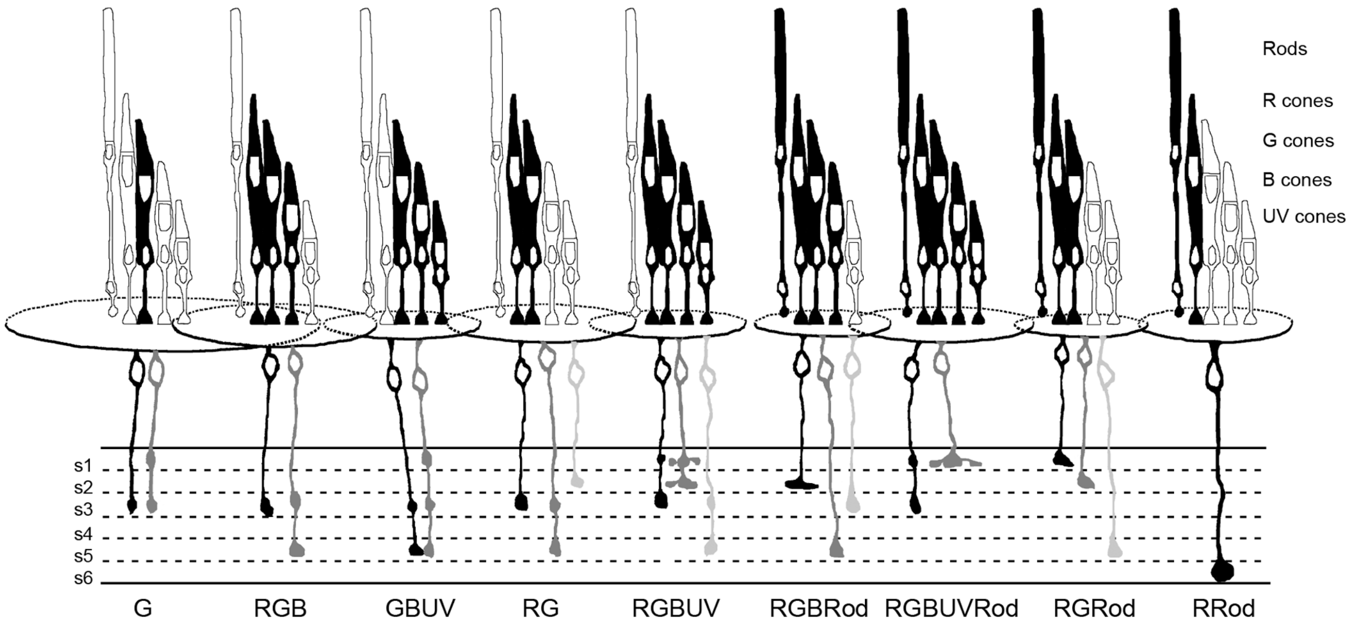

Figure 8.

Summary diagram of the photoreceptor connections, relative average dendritic spread, soma size and depth, and major axonal stratification patterns of the 9 common bipolar cell connectivity subtypes. The identities of the photoreceptors are indicated at the right. The particular receptors to which the different bipolar cells connect are black, and relative average dimensions of the bipolar cell dendritic fields are indicated by the overlapping ellipses. The relative average soma sizes and depths are also indicated. For each bipolar cell connectivity type, the most commonly observed cell with regard to axonal stratification is black, the next most common in gray and the third in silver. See text for details

Table 1

Stratification Analysis of the 308 Bipolar Cells of the 9 Common Connectivity Subtypes.

Mono-stratified				Bi-stratified				Tri-stratified			
	All	**Cone**	**Mixed**		**All**	**Cone**	**Mixed**		**All**	**Cone**	**Mixed**
s1	36	4	32	s1s2	12	5	7	s1s2s3	8	1	7
s2	41	11	30	s1s3	31	14	17	s1s3s4	1	1	0
s3	41	25	16	s1s4	1	1	0	s1s3s5	7	7	0
s4	15	5	10	s2s3	4	4	0	s1s3s6	2	0	2
s5	28	7	21	s2s4	3	2	1	s1s4s5	1	0	1
s6	23	1	22	s2s5	1	1	0	s2s3s4	2	1	1
				s3s4	5	3	2	s2s3s5	1	1	0
				s3s5	31	23	8	s3s4s5	1	0	1
				s3s6	3	2	1	s3s4s6	2	1	1
				s4s5	2	0	2				
				s4s6	5	4	1				
				s5s6	1	1	0				
Subtotal	184	57	144	Subtotal	99	60	39	Subtotal	25	12	13

NIH-PA Author Manuscript

NIH-PA Author Manuscript

Table 2

Distribution in the Major Axonal Stratification Patterns of the 9 Common Connectivity Subtypes

	Subtotal	G	RGB	GBUV	RG	RGBUV	RGBRod	RGBUVRod	RGRod	RRod
s1	36				2	2	4	5	23	
s2	41	2	1	1	4	3	11	3	16	
s3	41	6	8	2	6	3	7	2	7	
s4	15		1		2	2	4	2	4	
s5	28		2	1	4		7	2	12	
s6	23					1	1	1	2	18
s1s2	12					5	3	4		
s1s3	31	5		2		7		17		
s3s5	31		4	10	5	4	2	1	5	
s1s2s3	8			1			1	4	2	
s1s3s5	7			6		1				
Total	273	13	16	23	23	28	40	41	71	18

Table 3

Morphometry of the 308 Bipolar Cells of the 9 Common Connectivity Subtypes.

	Dendritic Spread Area (μm^2)				Soma Size (μm^2)				Soma Depth (μm)			
Subtype	**All**	**OFF**	**ON**	**ON-OFF**	**All**	**OFF**	**ON**	**ON-OFF**	**All**	**OFF**	**ON**	**ON-OFF**
G	$2610 \pm 2196^{\Delta}$	2610 ± 2196	n/a	n/a	43 ± 14	43 ± 14	n/a	n/a	13 ± 3	13 ± 3	n/a	n/a
GBUV	555 ± 374	$777 \pm 463^{*}$	$230 \pm 12^{*\#}$	$536 \pm 338^{\#}$	37 ± 9	42 ± 9	38 ± 5	35 ± 9	$16 \pm 5^{\Delta}$	15 ± 4	19 ± 5	15 ± 5
RG	703 ± 400	787 ± 434	565 ± 379	704 ± 369	37 ± 8	36 ± 9	39 ± 6	38 ± 8	12 ± 4	11 ± 3	15 ± 6	10 ± 1
RGB	780 ± 351	$591 \pm 373^{*}$	870 ± 187	$971 \pm 294^{*}$	$35 \pm 8^{\Delta}$	36 ± 9	38 ± 8	33 ± 7	12 ± 3	12 ± 4	11 ± 2	12 ± 3
RGBUV	558 ± 331	572 ± 322	816 ± 492	551 ± 429	36 ± 10	35 ± 8	48 ± 18	36 ± 8	12 ± 4	11 ± 4	14 ± 5	14 ± 5
RGBRod	$445 \pm 240^{\Delta}$	381 ± 196	507 ± 257	603 ± 330	39 ± 10	$40 \pm 10^{*}$	39 ± 9	$32 \pm 6^{*}$	13 ± 3	12 ± 3	13 ± 4	15 ± 5
RGBUVRod	658 ± 401	599 ± 300	$463 \pm 353^{*}$	$1196 \pm 571^{*}$	40 ± 9	41 ± 9	37 ± 8	41 ± 10	11 ± 4	11 ± 2	15 ± 8	11 ± 4
RGRod	$431 \pm 243^{\Delta}$	395 ± 167	477 ± 322	600 ± 379	39 ± 9	37 ± 8	39 ± 9	47 ± 15	$12 \pm 4^{\Delta}$	11 ± 3	13 ± 4	14 ± 4
RRod	608 ± 220	n/a	608 ± 220	n/a	$53 \pm 11^{\Delta}$	n/a	53 ± 11	n/a	$14 \pm 2^{\Delta}$	n/a	14 ± 2	n/a
Subtotal	657 ± 723	693 ± 908	$548 \pm 306^{*}$	$688 \pm 424^{*}$	39 ± 10	$39 \pm 10^{*}$	$43 \pm 12^{*\#}$	$37 \pm 10^{\#}$	12 ± 4	$11 \pm 3^{*\#}$	$14 \pm 4^{*}$	$13 \pm 5^{\#}$

n/a, not applicable;

$^{\Delta,*,\#}$p<0.05 (Student *t*-test);

$^{\Delta}$bipolar cells of a connectivity subtype were compared with those of the other 8 subtypes;

*OFF, ON, and ON-OFF bipolar cells of a connectivity subtype or the 308 bipolar cells were compared.

$^{\#}$OFF, ON, and ON-OFF bipolar cells of a connectivity subtype or the 308 bipolar cells were compared.

NIH-PA Author Manuscript

NIH-PA Author Manuscript

Table 4

Photoreceptor Connection Counts and the Cone Count/Dendritic Spread Area Ratios for the 9 Common Connectivity Subtypes.

	All					Cone Count				Cone Count/Dendritic Spread Area			
Subtype	R	G	B	UV	Rod	All	OFF	ON	ON-OFF	All	OFF	ON	ON-OFF
G	0	15 ± 6	0	0	0	15 ± 6	15 ± 6	n/a	n/a	0.01 ± 0.00$^{\Delta}$	0.01 ± 0.00	n/a	n/a
GBUV	0	8 ± 6	4 ± 3	5 ± 3	0	17 ± 8	20 ± 8 *	10 ± 1 $^{*\#}$	17 ± 8$^{\#}$	0.04 ± 0.02	0.04 ± 0.02	0.04 ± 0.01	0.04 ± 0.02
RG	7 ± 4	9 ± 4	0	0	0	16 ± 6	16 ± 6	16 ± 5	17 ± 7	0.03 ± 0.02$^{\Delta}$	0.02 ± 0.01	0.05 ± 0.03	0.03 ± 0.01
RGB	7 ± 4	11 ± 7	3 ± 2	0	0	21 ± 6$^{\Delta}$	19 ± 6	23 ± 11	21 ± 2	0.03 ± 0.02	0.04 ± 0.02 *	0.03 ± 0.02	0.02 ± 0.01 *
RGBUV	5 ± 3	7 ± 3	4 ± 3	4 ± 2	0	21 ± 7$^{\Delta}$	21 ± 7	22 ± 13	20 ± 7	0.05 ± 0.03$^{\Delta}$	0.05 ± 0.02	0.03 ± 0.01	0.06 ± 0.04
RGBRod	8 ± 3	8 ± 3	2 ± 1	0	9 ± 8	17 ± 6	16 ± 5 *	20 ± 6 $^{*\#}$	14 ± 4$^{\#}$	0.04 ± 0.02$^{\Delta}$	0.05 ± 0.02	0.04 ± 0.01	0.03 ± 0.02
RGBUVRod	7 ± 3	9 ± 5	4 ± 3	4 ± 2	6 ± 6	24 ± 9$^{\Delta}$	26 ± 8	15 ± 5	25 ± 9	0.05 ± 0.02$^{\Delta}$	0.05 ± 0.02 *	0.05 ± 0.03	0.02 ± 0.01 *
RGRod	8 ± 3	7 ± 3	0	0	9 ± 9	15 ± 5$^{\Delta}$	15 ± 4	15 ± 4	15 ± 7	0.04 ± 0.01	0.04 ± 0.01	0.04 ± 0.02	0.03 ± 0.02
RRod	9 ± 2	0	0	0	55 ± 26	9 ± 2$^{\Delta}$	n/a	9 ± 2	n/a	0.02 ± 0.00$^{\Delta}$	n/a	0.02 ± 0.00	n/a
Total	6 ± 4	8 ± 5	2 ± 2	1 ± 3	8 ± 15	18 ± 7	18 ± 7 *	15 ± 7 $^{*\#}$	18 ± 7$^{\#}$	0.04 ± 0.02	0.04 ± 0.02	0.04 ± 0.02	0.03 ± 0.02

n/a, not applicable;

$^{\Delta,*,\#}$p<0.05 (Student *t*-test);

$^{\Delta}$bipolar cells of a connectivity subtype were compared with those of the other 8 subtypes;

*OFF, ON, and ON-OFF bipolar cells of a connectivity subtype or the 308 bipolar cells were compared.

$^{\#}$OFF, ON, and ON-OFF bipolar cells of a connectivity subtype or the 308 bipolar cells were compared.